

Nanoscale Roughness on Metal Surfaces Can Increase Tip-Enhanced Raman Scattering by an Order of Magnitude

Weihua Zhang,[†] Xudong Cui,[‡] Boon-Siang Yeo,[†] Thomas Schmid,[†]
Christian Hafner,[‡] and Renato Zenobi^{*,†}

Department of Chemistry and Applied Biosciences, ETH Zurich, 8093 Zurich, Switzerland, and Laboratory for Electromagnetic Fields and Microwave Electronics, ETH Zurich, 8092 Zurich, Switzerland

Received March 15, 2007; Revised Manuscript Received April 10, 2007

ABSTRACT

We studied the influence of nanosteps on signal intensity in gap-mode tip-enhanced Raman spectroscopy (TERS). A benzenethiol monolayer adsorbed on an Au substrate was investigated. The correlation between the TERS signal and the local topography on the substrate shows that a 2 nm high sharp step on the Au surface can significantly increase the enhancement. Furthermore, theoretical models were built, and the numerical simulation results were consistent with our experimental results. The findings provide evidence that nanoscale roughness can play a crucial role in the “hot sites” corresponding to single-molecule surface-enhanced Raman spectroscopy (SERS).

Recently, single-molecule gap-mode tip-enhanced Raman spectroscopy (TERS) has been demonstrated by several groups independently.^{1–3} This provides an unprecedented opportunity for molecular identification and analysis with nanoscale spatial resolution in many areas such as catalysis, bioscience, nanomaterials, etc.^{4–6} TERS employs a sharp metal tip to create a “hot site”: to excite the localized surface plasmons (LSPs) and consequently enhance the electromagnetic field and Raman signals in the vicinity of the tip apex.^{6–9} Especially, when the substrate is a metal, the field enhancement can be further increased and reach 10² times.^{10,11} This is analogous to the case of using gaps in nanoparticle pairs or clusters to create “hot sites” in single-molecule surface-enhanced Raman spectroscopy (SERS) experiments.^{12,13} However, metal substrates may also cause a problem, namely topography-induced artifacts in TERS mapping. Unlike transmission mode TERS, in which the substrate is transparent and does not strongly interact with the tip from the optical point of view, the metal substrate used in gap-mode TERS couples with the light and supports the LSPs together with the tip.¹⁰ Consequently, the roughness on the substrate may significantly modulate the Raman signal and convolute topographical information with optical infor-

mation. We therefore decided to study how the corrugation of the substrate, which may be only a few nanometers, influences the enhancement.

Studying the influences of these small features on the field enhancement is not only important for understanding gap-mode TERS in view of imaging applications but also increases our knowledge about the “hot sites” in SERS. Currently, even for the best studied “hot site” (the nanogap between nanoparticle pairs), only simplified models composed of spheres or other ideal geometrical shapes were considered or simulated.^{14–16} This is different from reality, where the particle shape is never ideal.¹⁴ Therefore, investigating to what extent these simplified models are correct is also of interest. If subtle structures can significantly change the enhancement, more sophisticated models will be needed to describe and understand the properties of the “hot sites”.

As far as we know, the role small structures play in determining the enhancement is still poorly known despite the potentially huge effect for SERS/TERS. Several reasons, such as the lack of experimental methods for investigating small structures, the complexity of numerical simulations, and the lack of knowledge about the optical properties of the metal nanostructures, are responsible for this situation. There are only two possibilities to investigate structures down to 1 nm experimentally: transmission electron microscopy (TEM) and scanning probe microscopy (SPM). Because of practical difficulties, no SERS experiment was ever done

* Corresponding author. E-mail: zenobi@org.chem.ethz.ch. Telephone: +41 44 632 4376. Fax: +41 44 632 1292.

[†] Department of Chemistry and Applied Biosciences, ETH Zurich.

[‡] Laboratory for Electromagnetic Fields and Microwave Electronics, ETH Zurich.

with TEM monitoring. In the area of SPM, the scanning near-field optical microscope (SNOM), a hybrid technique of SPM and optical microscope, has been employed to investigate “hot sites”.^{17,18} Unfortunately, its limited optical resolution prevents it from successfully observing structures smaller than 50 nm. Likewise, simulations for small metal structures are also difficult. For the commonly used methods, such as the finite element method (FEM), the finite-difference time-domain (FDTD) method, etc., smaller structures need a finer discretization of the calculated space, and larger matrixes and larger storage are required. Moreover, the current simulation methods have a characteristic weakness: they cannot correctly handle the surface effect of metal. When the size of a metal structure is smaller than 5 nm, the surface will strongly modulate the response of the conduction electrons to the external electromagnetic field, and as a result, the bulk optical properties will not be correct any longer.^{19,20} Recent measurements of single gold nanospheres with 10 and 15 nm diameter show good agreement in the real part of the permittivity over the observed wavelength range (480–610 nm) and small differences in the imaginary part for wavelengths below 520 nm.²¹ Above 610 nm wavelength, the measured imaginary part of the 10 nm sphere is considerably below the one of the 15 nm sphere. It is likely that this surprising result is due to measurement problems. At our operating wavelength (633 nm), we therefore expect that the macroscopic description of nanospheres with radii of 5 nm or even less is still sufficiently accurate.

In this letter, we investigate the correlation between the nanocorrugation and the TERS intensity experimentally. We also phenomenologically built models and simulated how those nanostructures influence the electromagnetic field distribution. Both the experimental and simulation results show that a 2 nm step can significantly increase the enhancement in TERS. It affords us an opportunity to peer at this unexplored size range of metal structures and increases our knowledge of the “hot sites”.

The detailed description of the instrument used in this work can be found in our previous work.¹ Briefly, it is a combination of a homemade side-illuminated micro-Raman system and a STM system (Easyscan, Nanosurf). Ag tips were used in this work. They were fabricated by electrochemically etching an Ag wire (99.99%, Aldrich).²² To improve the sharpness of the Ag tips, a home-built electronic circuit was used to switch off the etching current automatically.²³ The radius of curvature of the tip apex can be controlled to be smaller than 50 nm after carefully setting the etching parameters.¹ During the measurement, the constant current mode of the STM was used with a 1.0 nA tunneling current and a –0.1 V bias voltage. The tip–sample distance is approximately 1 nm. All experiments were performed at ambient conditions.

The sample used in this work was a benzenethiol monolayer on a planar Au substrate. The Au substrate was made by evaporating 99.99% Au onto freshly cleaved mica in high vacuum. The monolayer was produced by soaking the Au substrate in a 10^{-2} M benzenethiol solution for 4 min. The unbound molecules were removed by thoroughly rinsing with

ethanol. Benzenethiol was chosen in this work because it forms a homogeneous self-assembled monolayer on an Au surface.²⁴ This is important for obtaining reliable reference data on the electric field enhancement and its spatial variation. Furthermore, the TERS signal of benzenethiol was relatively stable. No temporal fluctuations were observed in this work.

The experiment was done in the following way. First, a topography image was recorded to identify an interesting area where sharp edges are present. Then, a TERS line scan was recorded across these edges. After that, the tip was checked using a clean Au substrate to ensure that there was no contamination on the tip.

This experiment requires excellent stability for the STM. The drift of the system must be controlled to within ≤ 2 nm during the measurements, otherwise the data would be meaningless because the minimum step of the TERS mappings chosen was only 5 nm. To decrease the drift, two measures were taken: (1) the length from the tip apex to the tip holder was shortened from 10 to 2 mm, which caused the drift induced by the stress-relaxation of the tip shaft to be significantly decreased; (2) the scanner was always fully warmed up by long prescanning. Furthermore, in our experiments, topography images were scanned before and after the TERS measurements to guarantee that the drift was small enough.

For the simulations, the multiple multipole program (MMP) was used.²⁵ MMP is a semianalytic frequency domain method in which the electric field is expressed by a series of analytical solutions of Maxwell’s equations and solved by using the boundary conditions between different domains by means of a sophisticated error minimization technique. Its semianalytic property makes it precise and appropriate for the near-field related questions.²⁶

During the simulation, a plane wave, at an incident angle of 45° with respect to the surface normal, was used as the light source. Its wavelength was 633 nm. The corresponding permittivities of Ag and Au are $-18.12989 + 0.4836577i$ and $-11.71867 + 1.263433i$, respectively.²⁷

“Hot edges” in the Gap. The experimental results indicate that a sharp nanostep (≥ 2 nm) of the Au surface can significantly increase the Raman signal, while significantly coarser surface corrugation or smaller steps cannot. Figure 1 is an example for this. The TERS signal is by far the highest when the tip is on a sharp step of 2 nm height (position 2). On the contrary, the signal on a broad bump (positions 7, 8, and 9) or on a 1 nm step (position 5) is much lower, comparable to the signal in flat areas.

One may argue that the step at position 2 shown in Figure 1b is not that sharp because the slope between position 2 and 3 is not steep. However, the topography obtained by STM is a convolution between the tip and the sample surface, an effect that does occur for samples that have some corrugation.²⁸ If the edge is sharper than the tip, the image will only represent the shape of the tip apex, as demonstrated in Figure 1d. To estimate the real morphology of the sample surface, the tip shape is needed. Because there is no experimental method to determine the shape of the tip apex

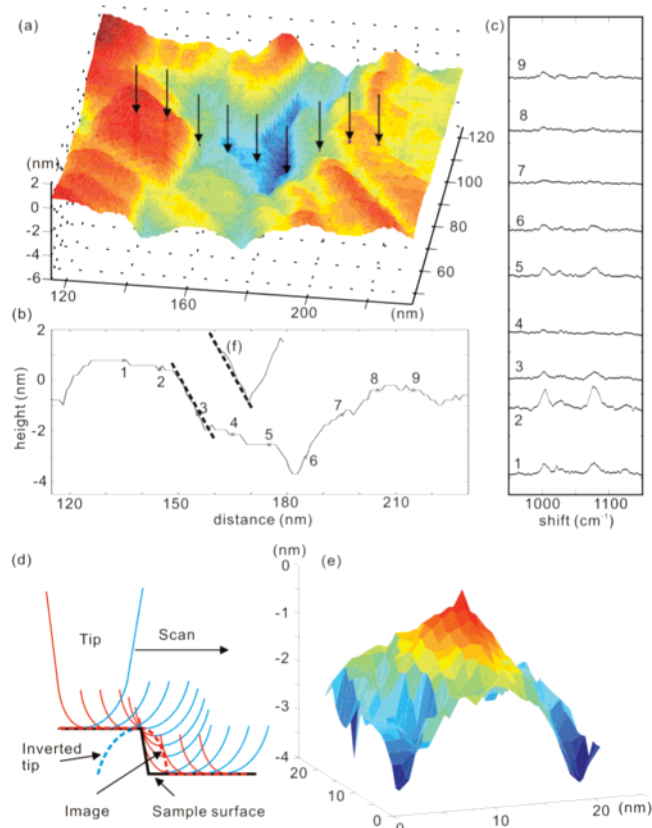


Figure 1. TERS mapping on a rough Au surface. An STM image of the sample is shown in (a). TERS data was collected at the positions indicated by the arrows. The cross section of the topography image is shown in (b), and the TERS collection sites are labeled with crosses. The corresponding TERS spectra are displayed in (c). The numbers denote the sites where the spectra were collected. The collection time for each spectrum was 30 s, and the laser power was 0.5 mW. Panel (d) is a cartoon showing that the STM image (dashed red line) only represents the tip shape if a sharp step is present on the sample surface (solid black line). The tips shape can be reconstructed from the image, and the result is shown in (e). The cross section of the tip (f) fits the edge at position 2 in panel (b) well. This implies that the step at position 2 is steeper than the case shown in the image.

with a precision better than 1 nm, we calculated the tip shape by using the blind reconstruction method, which estimates the bluntest possibility of the tip shape by using the topographical image.^{29,30} The result is shown in Figure 1e and f. We found that the tip shape fits the profile of at position 2 in Figure 1b well, thus this part of the STM topography is essentially the tip shape scanning the sharp corner on the sample surface, i.e., the real step is sharper than that.

Moreover, the increase of the enhancement is very sensitive to the relative position between the edge and the gap. Figure 2 is an example. It is also a TERS map but with a smaller step (5 nm) between neighboring measurement points. Similar to the result of Figure 1, the Raman intensity peaks at the sharpest corner (position 11). The interesting point here is that the Raman signal drops by ~ 10 times when the tip is only 5 nm away (position 12) from the edge. It implies that the formation of a “hot site” depends strongly on the relative position between the sharp corner and the gap.

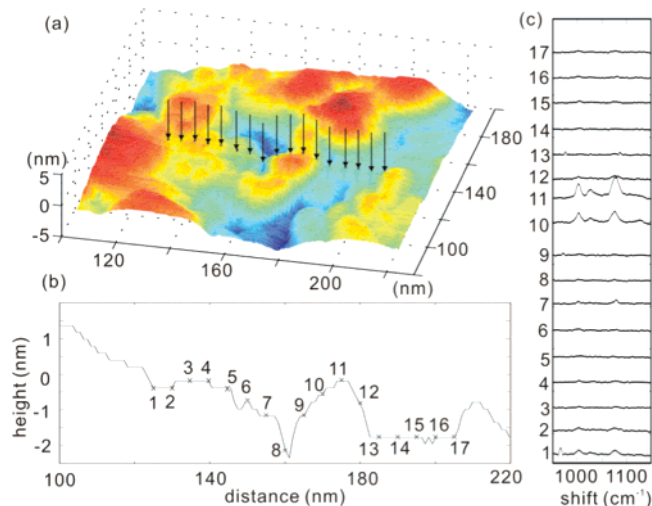


Figure 2. TERS mapping on a rough Au surface. An STM image of the sample is shown in (a). TERS data was collected at the positions indicated by the arrows. The cross section of the topography image is shown in (b), and the TERS collection sites are labeled with crosses. Panel (c) is the corresponding TERS sequence. The numbers denote the sites where the spectra were collected. The exposure time of each spectrum was 30 s, and the laser power was 0.5 mW.

Simulation. To understand the properties of the LSPs in the gap, a simplified 2D model was used to simulate our experiment (Figure 3): a 2D sphere is used as a tip and placed 1 nm above an infinite Au substrate. Three different substrates were simulated here: a flat substrate, a substrate with a sharp 90° step, or a slope. The height of these steps is 2 nm and the width of the slope is 20 nm to simulate the experimental result shown in Figure 1. All the “hard” corners (the joints of two straight lines) in the model are “softened” by small arcs. This is because the ideally sharp points are singularities and sometimes lead to nonphysical high field intensity.

Figure 3 shows the result of a simulation: The electric field is enhanced in the tip–sample gap. When a sharp step is present, the field enhancement is further increased by 1.6 times compared to the case of a smooth surface. The Raman enhancement can be derived from the field enhancement using the formula:³¹

$$A_{\text{Raman}} = A(v_L)^2 A(v_S)^2 \quad (1)$$

Here, $A(v_L)$ and $A(v_S)$ denote the field enhancement at the frequencies of the incident laser and scattered Raman light, respectively. Because the field enhancement at these two frequencies are approximately the same,¹⁰ formula 1 can be simplified to:

$$A_{\text{Raman}} \approx A(v_L)^4 \quad (2)$$

Hence, a sharp step can further enhance the Raman signal by more than 6 times. However, if the corrugation is coarser, the field enhancement, and consequently the Raman enhancement, will be similar to the case of a smooth substrate.

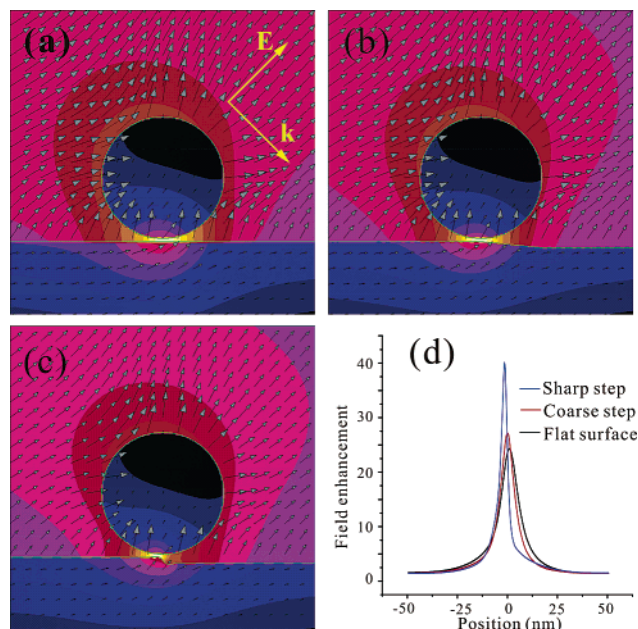


Figure 3. Simulation of the electric field distribution. Panels (a), (b), and (c) show the contours of $|E|$ for the following cases: a tip 1 nm above a flat surface, 1 nm above a broad step, and 1 nm above a straight step, respectively. Dark blue and bright yellow represent the lowest and highest field intensities, respectively. The factor between two neighboring lines is $2^{1/2}$. The direction and polarization of the excitation beam are illustrated in panel (a). The electric field is 45° with respect to the surface normal. The wavelength is 633 nm. The lateral distributions of the electric field enhancement in the plane of the tip–sample gap are demonstrated in (d).

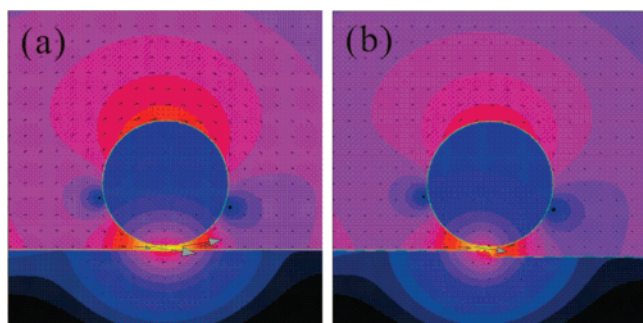


Figure 4. Contour of the Poynting vector distribution (the factor between two neighboring lines is $2^{1/2}$). Panel (a) and (b) correspond to the cases of the flat substrate and the sharp edge, respectively.

The findings of the simulation are consistent with our experimental results.

An interesting phenomenon shown in this simulation is that the presence of a step does not change the LSP modes of the system, as shown in Figure 4a and b, although the field is slightly distorted in the vicinity of the step. When the substrate is flat, the tip and the substrate couple with each other, and the p component (perpendicular to the substrate) of the electric field is significantly enhanced in the gap (Figure 3a and d). This is consistent with previous simulations and experiments. When an edge is right below the tip, surprisingly, the LSP modes are unchanged. Neither the field distribution surrounding the tip (Figure 3c) nor the

pattern of the Poynting vector (Figure 4b) is modified: no new modes are excited, and the polarization of the field in the gap is preserved. In other words, the gap mode is a relatively robust technique for TERS/SERS, although the existence of the subtle structures can tune the local field intensity.

We also calculated the cases with different tip–sample distance: 1.5 and 2.0 nm. Similar results were achieved except that the additional field enhancement by the sharp edge decreases slightly, from 1.68 times in the case of 1 nm tip–sample separation down to 1.53 and 1.48 times in the cases of 1.5 and 2.0 nm separation, respectively. Therefore, this step-induced electric field enhancement is not sensitive to tip–sample distance.

Where are the “Hot Sites”? According to the experimental and simulation results above, the “hot sites” rendering high field enhancement for single-molecule (SM) SERS can be a combination of a nanogap and a sharp structure. The shape of metal nanoparticles has been investigated before, and the results clearly show that the metal particles are polyhedrons with sharp edges rather than spheres.¹⁴ As mentioned above, the increase of the field enhancement is very sensitive to the relative position between the sharp edge and the gap. Hence, the possibility of forming a structure “hot” enough for SM-SERS is low. This is consistent with SM-SERS experiments: the “hot spots” are normally sparse on a SERS substrate.¹³

The results above differ somewhat from the results of a previous simulation by Xu et al.¹⁴ In their work, the field enhancement of a spherical pair and a polyhedron was compared, and the field enhancements of these two cases were found to be similar. However, this is not surprising because their models were different from ours and, as already discussed, the enhancement is sensitive to the geometrical parameters. What matters here is that the tiny structures can sometimes lead to a significant increase of the field enhancement, i.e., to understand nature of a “hot site”, geometrically ideal models are not sufficient, but the subtle structures must be considered.

Artifacts in TERS Mapping. Our results also show that a smooth Au substrate is necessary for TERS imaging. The local roughness of the metal substrate could introduce two types of artifacts into TERS mapping. First, small local morphological features can modulate the signal intensity by more than 10 times, as shown in Figure 2. Second, the roughness can induce a mismatch between the TERS map and the corresponding topography image. The simulation in Figure 3d shows that the distribution of the enhanced field is mainly concentrated on the upper terrace, not right below the tip. This asymmetric field distribution will deform the TERS image. This artifact can be further enhanced by the convolution effect of the tip shape, as shown in Figure 1d. If a blunt tip is used on a rough sample, the mismatch between the TERS map and the topographical image can be tens of nanometers, larger than the resolution of gap-mode TERS.

One of the potential applications of gap-mode TERS is catalysis: it is interesting to determine the reaction sites on

a metal catalysis substrate. However, the result shown in Figure 3 implies that mismatches between the TERS image and the corresponding topography image will occur if there are sharp structures. Thus, to obtain reliable data, a planar substrate without steep steps (corrugation <1 nm), which may not be catalytically active, is necessary.

In summary, we found that a sharp edge of only 2 nm height can induce a significant enhancement in gap-mode TERS mapping. This finding is also supported by electro-magnetic field simulations. The result suggests that a smooth substrate is necessary to avoid topographical artifacts in TERS maps. Moreover, it implies that sharp edges in the nanogaps may play an important role to form the “hot sites” in SM-SERS, providing a new possibility for designing high-performance nanostructures for surface-enhanced spectroscopy.

Acknowledgment. This project was supported by Gebert-Rüf Foundation (grant no. P-085/03) and the Deutsche Forschungsgemeinschaft (grant awarded to Thomas Schmid).

References

- (1) Zhang, W.; Yeo, B.; Schmid, T.; Zenobi, R. *J. Phys. Chem. C* **2007**, *111*, 1733.
- (2) Neacsu, C. C.; Dreyer, J.; Behr, N.; Raschke, M. B. *Phys. Rev. B* **2006**, *73*.
- (3) Domke, K. F.; Zhang, D.; Pettinger, B. *J. Am. Chem. Soc.* **2006**, *128*, 14721.
- (4) Ren, B.; Picardi, G.; Pettinger, B.; Schuster, R.; Ertl, G. *Angew. Chem., Int. Ed.* **2005**, *44*, 139.
- (5) Rasmussen, A.; Deckert, V. *J. Raman Spectrosc.* **2006**, *37*, 311.
- (6) Hartschuh, A.; Sanchez, E. J.; Xie, X. S.; Novotny, L. *Phys. Rev. Lett.* **2003**, *90*, 095503.
- (7) Zayats, A. V. *Opt. Commun.* **1999**, *161*, 156.
- (8) Hayazawa, N.; Inouye, Y.; Sekkat, Z.; Kawata, S. *Opt. Commun.* **2000**, *183*, 333.
- (9) Stöckle, R. M.; Suh, Y. D.; Deckert, V.; Zenobi, R. *Chem. Phys. Lett.* **2000**, *318*, 131.
- (10) Nottingher, I.; Elfick, A. *J. Phys. Chem. B* **2005**, *109*, 15699.
- (11) Pettinger, B.; Ren, B.; Picardi, G.; Schuster, R.; Ertl, G. *Phys. Rev. Lett.* **2004**, *92*.
- (12) Jiang, J.; Bosnick, K.; Maillard, M.; Brus, L. *J. Phys. Chem. B* **2003**, *107*, 9964.
- (13) Xu, H. X.; Bjerneld, E. J.; Kall, M.; Borjesson, L. *Phys. Rev. Lett.* **1999**, *83*, 4357.
- (14) Xu, H. X.; Aizpurua, J.; Kall, M.; Apell, P. *Phys. Rev. E* **2000**, *62*, 4318.
- (15) Gersten, J. I.; Nitzan, A. *Surf. Sci.* **1985**, *158*, 165.
- (16) Inoue, M.; Ohtaka, K. *J. Phys. Soc. Jpn.* **1983**, *52*, 3853.
- (17) Zhang, P.; Haslett, T. L.; Douketis, C.; Moskovits, M. *Phys. Rev. B* **1998**, *57*, 15513.
- (18) Tsai, D. P.; Kovacs, J.; Wang, Z. H.; Moskovits, M.; Shalae, V. M.; Suh, J. S.; Botet, R. *Phys. Rev. Lett.* **1994**, *72*, 4149.
- (19) Kreibig, U.; Voller, M. *Optical Properties of Metal Clusters*; Springer: Berlin, 1995.
- (20) Bohren, C. F.; Juffman, D. R. *Absorption and Scattering of Light by Small Particles*; John Wiley: New York, 1983.
- (21) Stoller, P.; Jacobsen, V.; Sandoghdar, V. *Opt. Lett.* **2006**, *31*, 2474.
- (22) Iwami, M.; Uehara, Y.; Ushioda, S. *Rev. Sci. Instrum.* **1998**, *69*, 4010.
- (23) Ibe, J. P.; Bey, P. P.; Brandow, S. L.; Brizzolara, R. A.; Burnham, N. A.; Dilella, D. P.; Lee, K. P.; Marrian, C. R. K.; Colton, R. J. *J. Vac. Sci. Technol., A* **1990**, *8*, 3570.
- (24) Wan, L. J.; Terashima, M.; Noda, H.; Osawa, M. *J. Phys. Chem. B* **2000**, *104*, 3563.
- (25) Hafner, C. *Post-Modern Electromagnetics Using Intelligent Maxwell Solvers*; John Wiley & Sons: New York, 1999.
- (26) Novotny, L.; Bian, R. X.; Xie, X. S. *Phys. Rev. Lett.* **1997**, *79*, 645.
- (27) Johnson, P. B.; Christy, R. W. *Phys. Rev. B* **1972**, *6*, 4370.
- (28) Hiesgen, R.; Meissner, D. *Ultramicroscopy* **1992**, *42*, 1403.
- (29) Williams, P. M.; Shakesheff, K. M.; Davies, M. C.; Jackson, D. E.; Roberts, C. J.; Tendler, S. J. B. *J. Vac. Sci. Technol., B* **1996**, *14*, 1557.
- (30) Villarrubia, J. S. *Surf. Sci.* **1994**, *321*, 287.
- (31) Kerker, M.; Wang, D. S.; Chew, H. *Appl. Opt.* **1980**, *19*, 3373.

NL070616N